Прилози, Одд. мат. тех. науки, МАНУ, **XXXII**, 45–66 (2011), с. 45–66
Contributions, Sec. Math. Tech. Sci., MANU, **XXXII**, 45–66 (2011), p. 45–66
ISSN 0351–3246
UDC: 550.348.013(497.115)"2002"

SOURCE MECHANISM AND SIZE OF THE 24 APRIL 2002 M_L 5.2 GNJILANE (KOSOVO) EARTHQUAKE

Vera Čejkovska, Lazo Pekevski, Dragana Černih

A b s t r a c t: The 24 April 2002 M_L 5.2 Gnjilane earthquake was studied first through inversion of the $S_g - L_g$ wave group displacement amplitude spectrum and *P*-nodal planes determination. The seismic moment, source spectrum corner frequency and Brune equivalent circular fault surface for this shock were obtained, respectively, as $M_0 = 6.48 \cdot 10^{16}$ N·m, $f_0 = 0.59$ Hz and $\Sigma_{s,eq} = 15.2$ km^2. The *P*-nodal planes for the four strongest aftershocks and the distribution of other aftershocks' epicentres were determined, too, and used in identifying the actual source mechanism of the main shock by a simple method that included also the vertical projections on the Earth's surface of the main shock $\Sigma_{s,eq}$ with the two main shock *P*-nodal planes as possible fault planes. It was found that the main shock was caused by a normal right lateral faulting in a plane which struck with an azimuth of 238° and dipped toward NNW under an angle of 22°. This faulting was associated with the shear stressed fault structure along the Pliocene-Quarternary sinking valley of Binačka Morava, and it led to activations of other ruptures as sources of a significant number of aftershocks.

Key words: seismic cycle, rupturing, source mechanism, faulting, seismic moment, fault surface, corner frequency

1. INTRODUCTION

On 24 April 2002, at 10:51 GMT, a moderate earthquake occurred near the town of Gnjilane in the region of Kosovo. The Seismological Observatory in Skopje (SKO) reported a local magnitude (M_L) of 5.2, and an epicentral location at 42.42 °N – 21.52 °E, the latter being positioned on the northern bank

of the river of Binačka Morava. The macroseismic effects of the earthquake spread throughout a big part of the Balkan Peninsula. The earthquake was followed by a sequence of shocks lasting for nearly a year. The four strongest aftershocks, all with local magnitudes $M_L = 4.1$ (SKO), occurred on 24 May 2002 at GMT 11h 24 min and 23 h 37 min, on 25 May 2002 at GMT 03 h 43 min and on 26 May at GMT 00 h 21 min. No significant foreshock activity was observed.

The tectonic conditions in Kosovo had been studied in details in the projects [1] and [2]. According to these studies, the territory of Kosovo is a region of confrontation of two first order tectonic structures, namely the Median (Serbo-Macedonian) Massif on East and the Massif of Dinarides on West. The latter contains second order tectonic units, and that are the Vardar zone (in the central part of Kosovo) and the Mirdita and Shar zones (in the southwestern part of Kosovo). The neotectonic activity in Kosovo is characterized by permanent uplifting of the terrain. It had passed a phase of flattening of the terrain through erosion and denudations (pre-orogenesis), which was proceeded by orogenesis, i.e. by differential, predominantly vertical movements of the first and second order tectonic structures under regional tectonic stresses that mainly resulted in an approximatively E-W oriented shear stressing. The orogenesis is still in progress, causing approximatively E-W oriented faultings, nearly perpendicular to the previous, NW-SE oriented faultings, thus leading to a formation of higher order tectonic structures, such as smaller uplifting units and sinking depressions. The present situation is given in Fig. 1.

T a b l e I

The parameters of the Balkans crustal model in [16]

Layer and depths of the boundary discontinuities km		Average density (ρ_0) 10^3 kg/m^3	Average shear modulus (μ_0) 10^{10} N/m^2 or 10^5 bar	P – wave average phase velocity (α_0) km/s	S – wave average phase velocity (β_0) km/s
Crust	Granite, 0–30	2.82	3.36	5.80	3.45
	Basalt, 30–40	3.02	4.48	6.65	3.85
Mantle		3.33	6.89	8.00	4.55

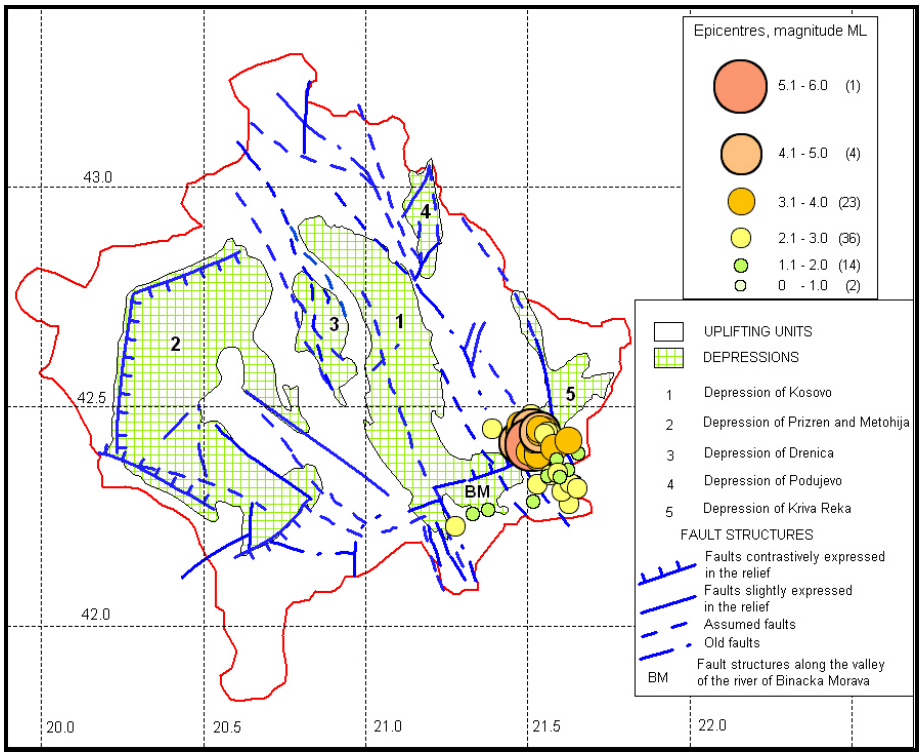

Fig. 1. Neotectonic map of the region of Kosovo and the 13 months period epicentres' distribution for the 24 April 2002 M_L 5.2 Gnjilane earthquake sequence. The neotectonic data from [1] and [2] were used. Note the following about the depressions: No. 1, 3 and 4 belong to the Vardar zone, No. 2 belongs to the Massif of Dinarides, and No. 5 belongs to the border region of the Vardar zone and the Serbo-Macedonian Massif

The recent seismic activity in the Kosovo region has been connected mainly to the approximatively E-W oriented faults, although the seismic activation of the NW-SE oriented faults has not been excluded. The source of the strongest earthquake observed in the last century (10 August 1921, 14 h 10 min GMT, M_L = 6.1) was associated with the fault structure along the approximatively E-W oriented valley of the river of Binačka Morava (e.g. [1], [2] and [3]). This sinking valley, which is a contact between the depression of Kriva Reka and the southern part of the depression of Kosovo, Fig. 1, was formed during the Eocene-Oligocene and was reactivated during the Upper Pliocene and Quaternary. The occurrence of moderate earthquakes (M_L values between 4.0 and 5.0) along this valley is relatively frequent [3].

The present study aims to find the actual source mechanism and size of the 24 April 2002 M_L 5.2 Gnjilane earthquake, as well as to sketch some characteristics of the whole corresponding seismic cycle. The results are expected to be important in hazard and risk assessment for moderate earthquakes in the Western Balkans.

2. THEORETICAL BACKGROUND

2.1. Seismic cycle

As it is derived from the uses of continuum mechanics, rupture mechanics and dislocation theory in studying earthquakes (see the basics [4], [5], [6], [7], [8], [9], and the recent developments [10], [11]), the most probable physical model of seismic cycle consists of four main phases: 1) increasing long-term tectonic stressing and gradual accumulation of homogeneous and cataclastic deformations in the so-called seismic source volume (a certain volume around the future main earthquake source – dynamic rupturing); 2) preseismic phase, i.e. unstable growth of the deformations in the seismic source volume, and, eventually, nucleation of a slow, non-dynamic main earthquake rupturing; 3) coseismic phase or main part of the rebound of the seismic source volume, i.e. nucleation, propagation and arrest of a dynamic main earthquake rupturing; the nucleation of this rupturing is referred to as the main earthquake hypocentre; 4) post-seismic phase, which represents all the phenomena after the arrest of the dynamic main earthquake rupturing, including the rebound of the seismic source volume through triggering or healing of smaller ruptures and cracks.) The main earthquake rupturing in the coseismic phase is described as *dynamic*, since it, under the tectonic stress, which can be assumed as constant during the short lasting of the earthquake, propagates with a velocity that increases rapidly, having the P wave velocity as upper limit. The short dynamic propagation of the main rupturing is followed by the process of its arresting, which can last much longer: the rupturing propagates slowly, interacting with similarly oriented major cracks and variously oriented small cracks, or stops with meeting significantly declined major cracks. The cracks which are triggered or healed during the seismic cycle are sources of smaller, adjacent earthquakes – foreshocks or aftershocks, depending on whether they occur before or after the main dynamic rupturing. The foci of the adjacent shocks occurred during the pre-seismic phase and the main dynamic rupturing arrest contour the final source surface for the main shock. Furthermore, according to all seismic

and non-seismic data, the long-term tectonic stressing in the first phase of the seismic cycle is most often a shear stressing, and, consequently, the most probable source model for the earthquakes is a dynamic faulting – a rupturing with relative slip of rupture's walls that propagates in a short time and with a velocity that increases rapidly, having the *S* wave velocity as upper limit. In addition, the most promising treatment of deep buried seismic sources is a modeling by means of dislocation theory.

In this study only seismological data for the 24 April 2002 M_L 5.2 Gnjilane earthquake sequence and tectonic data prior to the corresponding seismic cycle were used. Since no seismological data for foreshocks were available, it was possible to analyze directly only the coseismic and postseismic phases of the seismic cycle, and later on to infer conclusions about the other phases.

The starting point in this was the locating of sequence's hypocentres. Thus, the hypocentral locations for the main shock and 79 aftershocks from the period 24 May 2002 – 30 June 2003 were obtained using the programme HYPO71 [12] with the so-called Balkans crustal model (Table I, [13]). The P and S phases onset data from seismological stations with epicentral distances (Δ) from 40 to 1000 km were used ([14], [15], [16]). Data from at least five stations were required. The hypocentres of the main shock and the four strongest aftershocks were located with data from more than 30 stations. All obtained 80 hypocentral locations were in the granite layer of the crustal model presented in Table I (see the Appendix). It is important to mention this here, since such position of the main shock hypocentre was used in the theoretical formulation of the next step of the investigation.

2.2. Determination of the size of the main shock

An inversion of a part of the far-field (F) displacement amplitude spectrum (A^F) of the main shock was done in order to determine the size of the shock, i.e. the corresponding seismic moment (M_0), source spectrum corner frequency (f_0) and final fault surface (Σ_s). The $S_g - L_g$ wave group from the vertical component of the main shock digital record obtained at the station in Bitola (BIA, 41.02°N. 21.32°E) was used in the inversion. This record was obtained on an electromagnetic short-period Kinemetrics seismometer (SS-1) with a Kinemetrics digital 16-bits recorder (SSR), the latter working at a sampling rate of 100 Hz, and with low-cut 0.01 Hz and high-cut 50 Hz filters.

The theoretical shape of the analyzed displacement amplitude spectrum A^F was represented by

$$A^F = A_s^F \cdot G \cdot V \cdot \left|T_{\text{instr.}}\right|, \tag{1}$$

where A_s^F is the source term, G is the wave geometrical spreading factor, V is the wave anelastic attenuation and $\left|T_{\text{instr.}}\right|$ are the effects of the frequency (f) response function of the recording equipment, $T_{\text{instr.}} = T_{\text{instr.}}(f)$. The terms A_s^F, G and V were postulated only for the granite crustal layer, since the studied source, as mentioned above, was found to be located in that layer, and since S_g and L_g waves spread only in that layer. The model of geometrical spreading of S_g and L_g waves suggested in [17], [18] and [19] was used, with adoptions that fit the geomorphologic and seismotectonic conditions along the analyzed seismic path Gnjilane – Bitola: 1) the granite crustal layer was homogenized following the scheme from Table I; 2) the S_g and L_g waves were treated as one type of waves, which exhibit transition from spherical to cylindrical spreading at hypocentral (Herrman-Kijko) distance $R_{H,0} = 80\,\text{km}$ (the latter is a threshold of occurance of the L_g phase on the territory of the Republic of Macedonia and surrounding areas, [20]); 3) the average S wave phase velocity in granite crustal layer from Table I ($\beta_0 = 3.45$ km/s) was ascribed to both S_g and L_g wave phase velocities; 4) the spreading term G was taken as

$$G = G(R_{H,0}, R_H)^{-1/2}, \quad R_{H,0} = 80 \text{ km} \tag{2}$$

(the model from [17], [18] and [19] for hypocentral distances $R_H > R_{H,0}$). V was taken with constant and frequency independent quality factor $Q = 56$, a value obtained in [21] as an average for S and L_g waves within the Shar-Pelister (West Macedonia) seismic zone, through which the analyzed seismic path Gnjilane – Bitola spreads:

$$V = V(R_H, f) = \exp\left(-\pi \cdot f \cdot R_H / \beta_0 \cdot Q\right), \ \beta_0 = 3.45 \text{ km/s}, \ Q = 56. \tag{3}$$

According to the previous tectonic data (Section 1), the seismic source was treated as a faulting, and the generalized Brune shear dislocation source model (e.g., [22], [23]) was used for A_s^F in eq. (1), with specifics that corre-

sponded to the already mentioned location of the source in the granite layer of the crustal model presented in Table I:

$$A_s^F = \Omega_0 \cdot \left[1 + (f\ / f_0)^2\right]^{-\gamma/2}, \tag{a}$$

with

$$\Omega_0 = \frac{M_0 \cdot < F^{FS} >}{4\pi \cdot \rho_0 \cdot \beta_0^3} = \frac{M_0 \cdot 0.6324}{4\pi \cdot \rho_0 \cdot \beta_0^3}, \tag{b}$$

$$R_B = 2.34 \cdot \beta_0 / 2\pi \cdot f_0, \tag{c}$$

$$\rho_0 = 2.82 \cdot 10^3 \text{ kg/m}^3, \ \beta_0 = 3.45 \text{ km/s}. \tag{4}$$

Ω_0 is the source spectrum low-frequency part, M_0 is the seismic moment, $<F^{FS}>$ = 0.6324 is the RMS for *S* or L_g wave radiation pattern from the original Brune model ([24], [25]), and ρ_0 and β_0 are, respectively, the density and the *S* or L_g wave phase velocity in the vicinity of the real fault. The term $\left[1 + (f / f_0)^2\right]^{-\gamma/2}$ is the high-frequency part of the source spectrum, with fall-off exponent γ as a parameter, and f_0 is the source spectrum corner frequency that is due to the finite rise time of the dislocation proposed in the model. As in the original Brune model, R_B is the radius of the static circular fault surface $(\Sigma_{s,eq.})$ which is equivalent to the real final fault surface Σ_s.

The inversion was done with the seismological software SEISAN 8.2, [26], by fitting the observed spectrum with the theoretical spectrum A^F in the plane $\left[\lg f, \lg(A_s^F \cdot G)\right]$. The original SSR digital record of the main shock was converted into the SEISAN format, and then corrected for $|T_{\text{instr.}}|$ and V (following eq. 3). A time window of 15.7 s, which included the entire durations of both S_g and L_g phases on the record's vertical component, was chosen for the fitting. Outputs of the best fitting were obtained as $OM \equiv \lg(\Omega_0 \cdot G)$ and f_0, Fig. 2, and they were used to estimate the M_0 and R_B following the eqs. (4b) and (4c). The estimated R_B was used to obtain $\Sigma_{s,eq.}$ as $\Sigma_{s,eq.} = \pi \cdot R_B^2$.

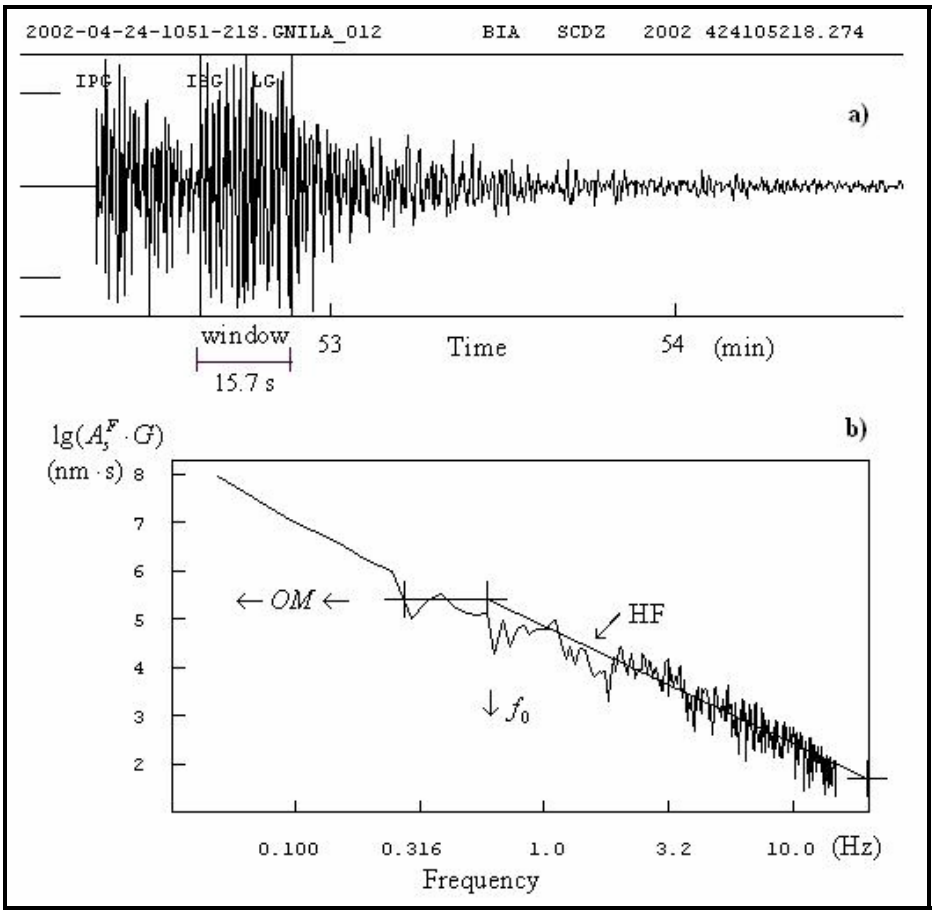

Fig. 2. a) The 16 bit SSR record of the 24 April 2002 M_L 5.2 Gnjilane earthquake on the vertical component of the short-period electromagnetic SS-1 seismometer at the station in Bitola (BIA), for which the epicentral distance and azimuth are Δ = 156.5 km and *Az* = 186°, respectively. The onsets of the seismic phases P_g, S_g and L_g are shown, too. **b)** The log-amplitude spectrum of the 15.7 s $S_g - L_g$ trace from the upper part of the figure, obtained in the SEISAN 8.2 software after corrections for the instrument response and anelastic attenuation. OM, HF and f_0 are respectively the low-frequency asymptote, the high-frequency asymptote and the corner frequency of the fitting theoretical log-amplitude spectrum. Other symbols are explained in the text

2.2. A method of identifying the actual source mechanism of the main shock

A simple method for distinguishing the real fault plane for the main shock from the two corresponding *P*-nodal planes, i.e. for identifying the actual source mechanism of this shock from the two source mechanisms suggested by the corresponding *P*-nodal solution was proposed and used here. The outline of the method is as follows.

It is assumed that the main shock dynamic faulting enters the final phase of its arrest with deflecting toward a major crack that is significantly declined from the faulting surface. This first deflecting major crack is a source of some of the strongest aftershocks near in time to the main shock, and it is found by comparison of the orientations of the *P*-nodal solutions for the main shock and strongest aftershocks. Furthermore, accordingly to the theory, it is taken that the final fault surface for the main shock is contoured by the hypocentres of the main shock, of the first deflecting aftershock and of all aftershocks occurred meanwhile. The dimensions of the distribution of the epicentres of all these shocks are then compared with the dimensions of the vertical projections on the Earth's surface of the main shock Brune equivalent circular fault surface $\Sigma_{S,eq.}$ for the cases when each of the two main shock *P*-nodal planes is taken as a fault plane (see the scheme of such projection in Fig. 3). This comparison allows identifying the actual fault plane and source mechanism for the main shock.

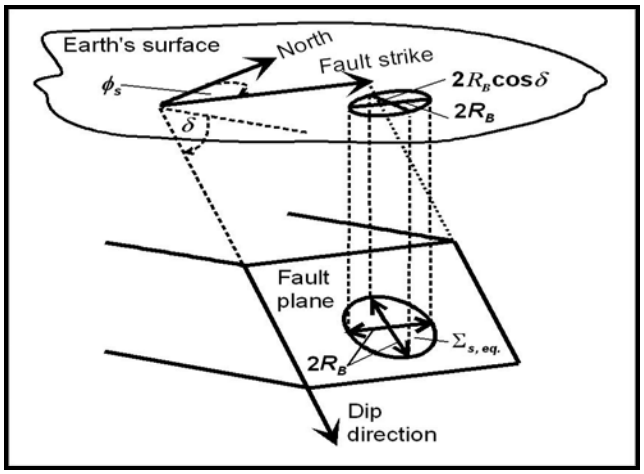

Fig. 3. Scheme of the vertical projection on the Earth's surface of a Brune equivalent circular fault surface $\Sigma_{S,eq}$ with a radius R_B. ϕ_s and δ are the strike azimuth and the dip angle of the fault plane

The proposed method seems to be a suitable one for moderate earthquakes, at which the directivity in radiation patterns is not well expressed, and therefore it can not be easily used in determining the actual source mechanism. However, the method can be applied only if there is at least one significant aftershock which source deflects the main shock dynamic faulting.

The *P*-nodal solutions for the main shock and the four strongest aftershocks were here obtained with the softwares FPFIT, FPPLOT and FPPAGE [27]. *P*-polarities data from more than 20 regional seismological stations were used for each solution.

3. RESULTS AND DISCUSSION

The obtained locations of the main shock and 79 aftershocks are presented in Fig.1 and in the Appendix, together with the corresponding M_L values obtained at SKO. The locations of the main shock and the four strongest aftershocks are also presented in Table II and in Fig. 4. The first 12 hours epicentres' distribution for the sequence is given in Fig. 5.

Outputs of the best fitting of the vertical component of the S_g and L_g wave displacement amplitude spectrum for the main shock observed at the station BIA with the theoretical spectrum A^F in the plane $\left[\lg f,\, \lg(A_s^F \cdot G)\right]$ in the software SEISAN 8.2 were found to be $OM \equiv \lg(\Omega_0 \cdot G) = 5.4$ and $f_0 = 0.59$ Hz, Fig. 2. Following eq. (4b), the seismic moment was estimated as

$$M_0 = \frac{10^{OM}}{0.6324} \cdot 4\pi \cdot \rho_0 \cdot \beta_0^3 \cdot R_{H,0}^{1/2} \cdot R_H^{1/2},$$
$$\rho_0 = 2.82 \cdot 10^3 \text{ kg/m}^3,\ \beta_0 = 3.45 \text{ km/s},\ R_{H,0} = 80 \text{ km},\ R_H = 157.2 \text{ km}, \tag{5}$$

where $R_H = 157.2$ km is the hypocentral distance for the station BIA. This gave the value $M_0 = 6.48 \cdot 10^{16}$ N·m. The replacing of $f_0 = 0.59$ Hz in eq. (4c) gave $R_B = 2.2$ km. Thus the circular fault surface which is equivalent to the real final fault surface is:

$$\Sigma_{s,eq.} = \pi \cdot R_B^2 = \pi \cdot (2.2\ \text{km})^2 = 15.2\ \text{km}^2 \approx 15\ \text{km}^2. \qquad (6)$$

The obtained *P*-nodal solutions for the main shock and the four strongest aftershocks are presented in Table II and in Fig. 4.

The vertical projections on the Earth's surface of the main shock Brune equivalent circular fault surface $\Sigma_{s,eq.}$, with the two main shock *P*-nodal planes as possible fault planes, are presented in Table III.

T a b l e II

Locations and P-nodal solutions for the 24 April 2002 M_L 5.2 Gnjilane earthquake and the four strongest aftershocks. H and h – hypocentral time and depth, φ and λ – epicentral latitude and longitude, M_L – local magnitude obtained at the Seismological Observatory in Skopje (SKO,41.97°N, 21.44°E); ϕ_s, δ and γ – strike azimuth, dip angle and hanging wall slip angle for a P-nodal plane; n-l-l – normal left lateral fault, n-r-l – normal right lateral fault

Shock						*P*-nodal plane I				*P*-nodal plane II			
Date DMY	*H* /GMT h : min : s	φ (°N)	λ (°E)	h (km)	M_L	$\phi_{s,I}$ (°)	δ_I (°)	γ_I (°)	Fault type	$\phi_{s,II}$ (°)	δ_{II} (°)	γ_{II} (°)	Fault type
24.04.2002 main shock	10:51:51.1	42.42	21.52	15	5.2	85 ENE	70 SSE	–80	n-l-l	238W SW	22 NNW	–116	n-r-l
24.04.2002 aftershock	11:24:22.2	42.43	21.51	18	4.1	95 ESE	60 SSW	–80	n-l-l	256 WSW	31 NNW	–107	n-r-l
24.04.2002 aftershock	23:37:57.5	42.44	21.54	20	4.1	143 SSE	71 WSW	–21	n-l-l	240 WSW	70 NNW	–160	n-r-l
25.04.2002 aftershock	03:43:34.8	42.45	21.51	18	4.1	110 ESE	70 SSW	–10	n-l-l	203 SSW	81 WNW	–160	n-r-l
26.04.2002 aftershock	00:21:31.7	42.42	21.47	12	4.1	106 ESE	15 SSW	–80	n-l-l	276 WNW	75 NNE	–93	n-r-l

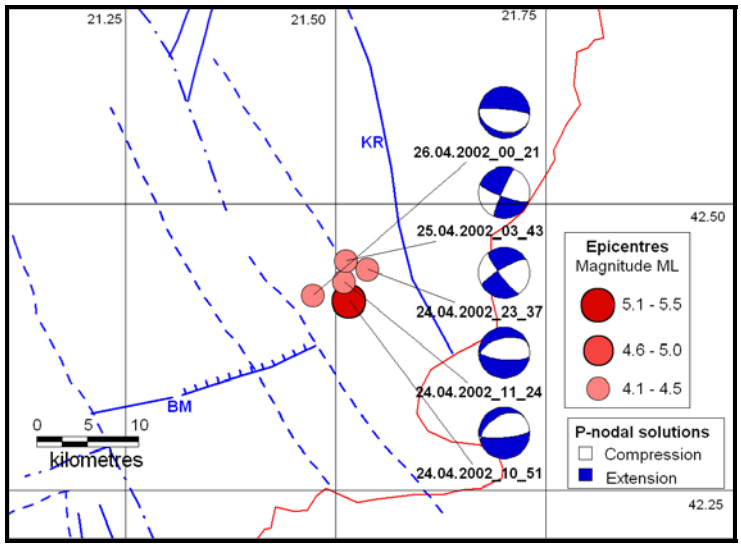

Fig. 4. Epicentral locations and *P*-nodal solutions for the 24 April 2002 M_L 52 Gnjilane earthquake and the four strongest aftershocks. BM and KR denote the faults of Binačka Morava and Kriva Reka

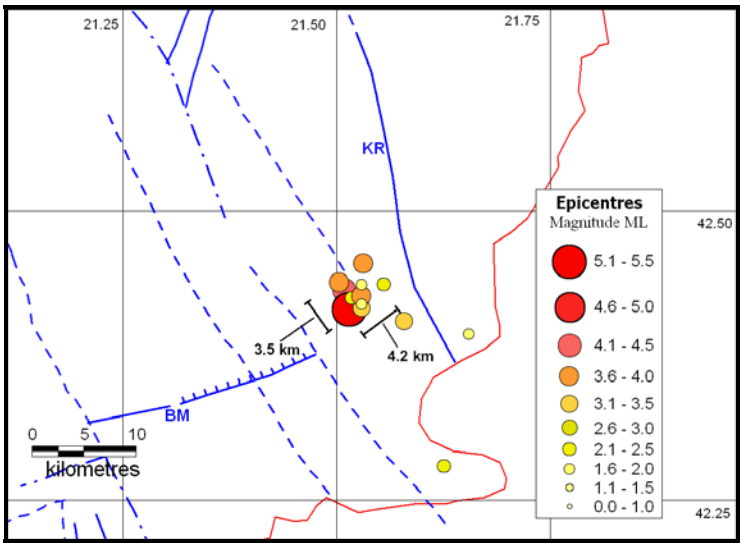

Fig. 5. The first 12 hours epicentres' distribution for the 24 April 2002 M_L 5.2 Gnjilane earthquake sequence. BM and KR denote the faults of Binačka Morava and Kriva Reka

T a b l e III

Vertical projections on the Earth's surface of the obtained Brune equivalent circular fault surface $\Sigma_{s,eq.}$ for the 24 April 2002 M_L 5.2 Gnjilane earthquake with the two corresponding P-nodal planes as possible fault planes (Table II). ϕ_s and δ – strike azimuth and dip angle of a fault (P-nodal) plane

Equivalent circular fault surface: radius $R_B = 2.2$ km, area $\Sigma_{s,eq.} = 15.2$ km^2	Vertical projection of $\Sigma_{s,eq.}$ on the Earth's surface		
	Ellipse		
	Major axis: $A_s = 2R_B$	Minor axis: $B_s = 2R_B \cos\delta$	Area: $S = A_s B_s \pi/4$
P-nodal plane I: $\phi_s = 85^0$, $\delta = 70^0$	4.4 km WSW–ENE	1.5 km NNW–SSE	5.2 km^2
P-nodal plane II: $\phi_s = 238^0$, $\delta = 22^0$	4.4 km ENE–WSW	4.1 km SSE–NNW	14.2 km^2

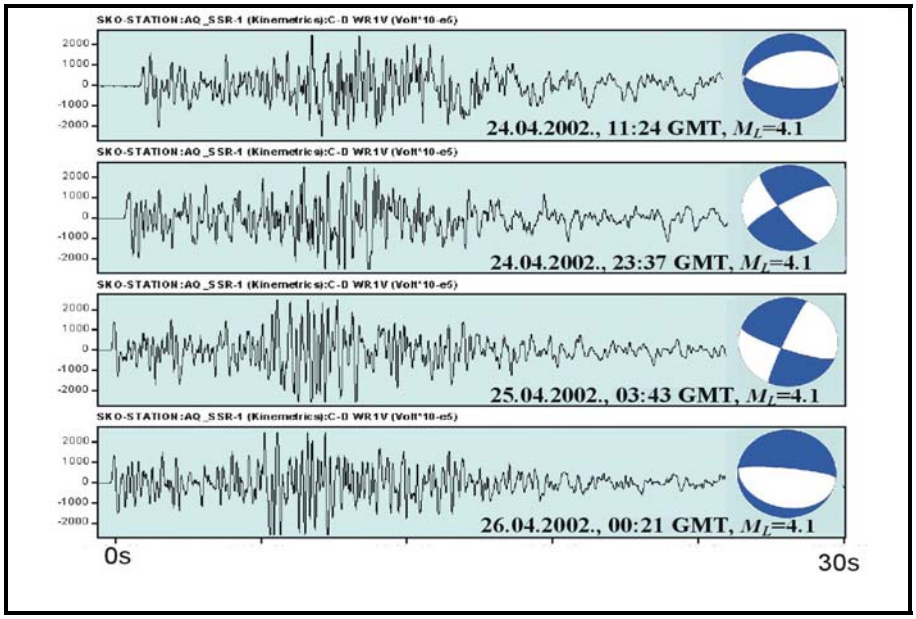

Fig. 6. The waveforms of the vertical components of the four strongest aftershocks of the 24 April 2002 *ML 5.2* Gnjilane earthquake recorded at the station in Skopje (SKO) and corresponding *P*-nodal solutions (beach balls). The differences in the waveforms suggest activations of different ruptures as sources of the shocks.

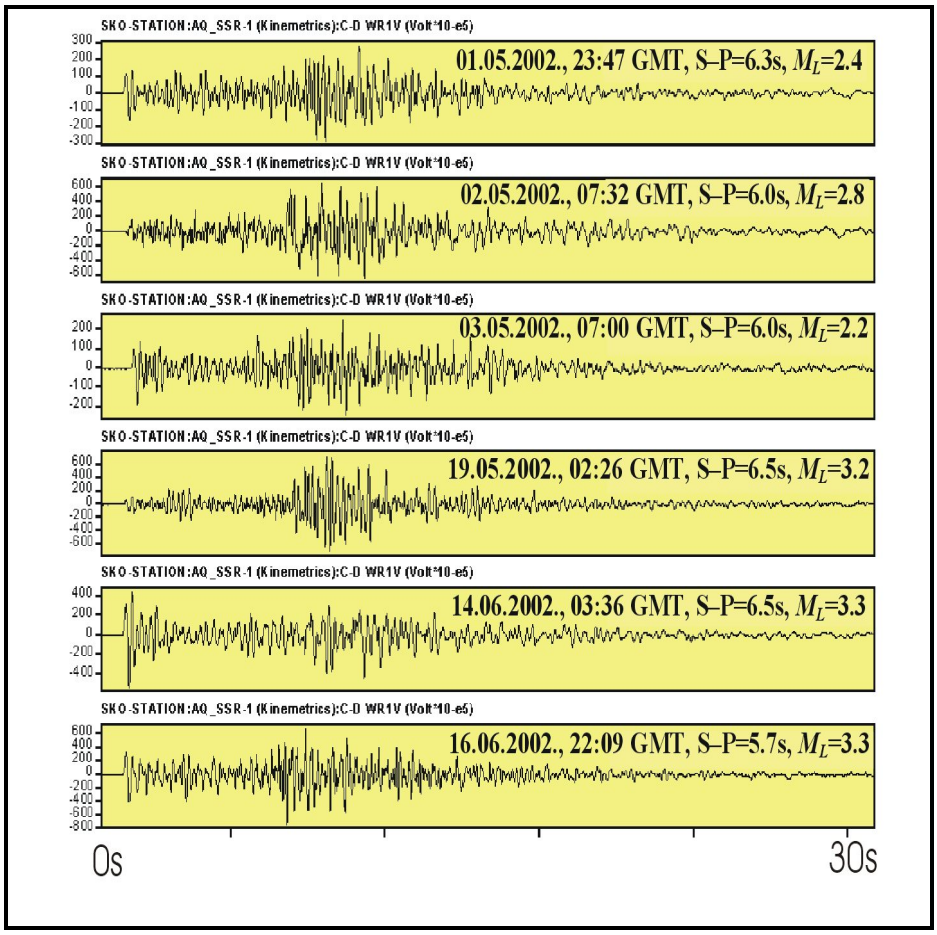

Fig 7. The waveforms of the vertical components of smaller aftershocks of the 24 April 2002 M_L 5.2 Gnjilane earthquake recorded at the station in Skopje (SKO). The differences in the waveforms point to activations of different ruptures as sources of the shocks.

As it can be seen from Fig. 4, the epicentre of the main shock was located between the faults of Binačka Morava and Kriva Reka. Thus, the simple identification of the fault that caused this shock is impossible. The same situation appears for the four strongest aftershocks (Fig. 4). Fig. 5 points that a certain migration of the aftershocks' epicentres in the wider area around the faults of Binačka Morava and Kriva Reka started within the first 12 hours of the se-

quence. This trend was kept on and led to the situation presented in Fig. 1. The latter shows that the epicentres' distribution of the studied earthquake sequence within a 13 months period spread throughout a wide area crisscrossed by fault ruptures. This distribution and the included wide range of aftershocks' local magnitudes (from 0.9 to 4.1, see the Appendix) mean that the post-seismic rebound for the studied earthquake included activations of variously oriented ruptures on various dimension levels (see Figs. 6 and 7). Therefore, it can be concluded that the phase of accumulation of deformations before the earthquake took place in a vast region.

The *P*-nodal solution for the main shock (Table II, Fig. 4.) clearly showed that the two *P*-nodal planes, i.e. the two possible fault planes for this shock, strike very similarly to the fault of Binačka Morava, although they dip under different angles ($\delta_{\mathrm{I}} = 70°$ toward SSE, and $\delta_{\mathrm{II}} = 22°$ toward NNW). On the other hand, declinations from these orientations appear in the *P*-nodal solutions for the four strongest aftershocks. Thus, the *P*-nodal solution for the 24 May 2002 GMT 11 h 24 min aftershock shows a slight declination, and the declination of the *P*-nodal solution for the 24 May 2002 GMT 23 h 37 min aftershock is the first one to be significant. The last trend continues, and the declinations of the *P*-nodal solutions for the 25 May 2002 GMT 03 h 43 min and the 26 May GMT 00 h 21 min aftershocks are significant too.

The above means that the arrest of the main shock dynamic faulting started with interactions with small cracks (sources of small aftershocks) or similarly oriented major cracks (as the one generating the 24 May 2002 GMT 11 h 24 min aftershock), and entered the final phase with meeting a significantly declined major crack – the source of the 24 May 2002 GMT 23 h 37 min aftershock. Consequently, it can be assumed that the final fault surface for the main shock was contoured by the hypocentres of the main shock and of the aftershocks occurred up to 24 May 2002 GMT 23 h 37 min, i.e. by the hypocentres of the shocks occurred approximatively within the first 12 hours of the sequence.

Following the method described in Section 2.3., the distribution of the epicentres of these aftershocks was further taken as a referential one in identifying the actual source mechanism for the main shock from its *P*-nodal solution. The area of this distribution was first estimated as an ellipse having axes equal to the measured major and minor linear dimensions of the distribution (Fig. 5), second – as a rectangle with sides equal to these dimensions. The average of the two obtained values was also found, Table IV.

T a b l e IV

Dimensions of the first 12 hours epicentres' distribution for the 24 April 2002 M_L 5.2 Gnjilane earthquake sequence

Epicentres' distribution	Major axis $A_{ep.}$	Minor axis $B_{ep.}$	Area, an ellipse $S_{ep.} = A_{ep.}B_{ep.}\pi/4$	Area, a rectangle $S_{ep.} = A_{ep.}B_{ep.}$	Area, average
The first 12 hours	4.2 km NE–SW	3.5 km SE-NW	11.5 km^2	14.7 km^2	13.1 km^2

As it follows from the comparison of the Tables III and IV, only the vertical projection on the Earth's surface of the main shock Brune equivalent circular fault surface $\Sigma_{s,eq.}$ with the second possible fault plane (*P*-nodal plane II) approximates the orientations and lengths of the major and minor linear dimensions of the first 12 hours shocks epicentres' distribution, as well as the planar extents of this distribution for all three considered cases: an elliptic area, a rectangular area or an average of both.

Thus it was possible to conclude that the main shock was caused by a normal right lateral faulting along a plane which struck with an azimuth of 238° and dipped toward NNW under an angle of 22°, which is the *P*-nodal plane II in the obtained *P*-nodal solution for this shock (Tables II). The fault surface had a maximal linear dimension of ≈ 4 km and an extent of ≈ 15 km^2, and that gave a seismic moment valued with $M_0 = 6.48 \cdot 10^{16}$ N·m According to the previous tectonic data, this faulting can be associated with the shear stressed fault structure along the Pliocene-Quaternary sinking valley of the river of Binačka Morava.

REFERENCES

[1] UNDP/UNESCO Survey of the Seismicity of the Balkan Region, UNESCO, Skopje**,** 1974.

[2] Dž. Orana, M. Arsovski, V. Mihailov, *Seizmotektonske karakteristike SAP Kosovo i njihov značaj za seizmičku rejonizaciju i ocene seizmičkog rizika,* Naučno-istraživački projekat, Tehnički fakultet – Priština i Institut za zemljotresno inženjerstvo i inženjersku seizmologiju – Skopje, 1985.

[3] Љ. Јордановски, Л. Пекевски, В. Чејковска, Д. Черних, Б. Христовски, Н. Василевски, *Основни карактеристики на сеизмичноста на територијата на*

Република Македонија, Универзитет „Св. Кирил и Методиј“, Природно-математички факултет, Сеизмолошка опсерваторија, Скопје, 1998.

[4] H. F. Reid, The elastic-rebound theory of earthquakes, *University of California Publ. Geol. Sci.,* 6 (1911) 413-444.

[5] Б. В. Костров, *Механика очага тектонического землетрясения,* Наука, Москва, 1975.

[6] М. А. Садовский, отв. ред., Сб. *Физика очага землетрясения,* Наука, Москва, 1975.

[7] М. А. Садовский, Б. И. Мячкин, отв. ред.-ы, Сб. *Физические процессы в очагах землетрясений*, Наука, Москва, 1980.

[8] Дж. Райс, *Механика очага землетрясения*, Мир, Москва, 1982.

[9] K. Kasahara, *Earthquake Mechanics*, Cambridge University Press, New York, 1981.

[10] S. Karato, Deformation of Earth Materials. An Introduction to the Rheology of Solid Earth, Cambridge University Press, 2008.

[11] E. Fukuyama, Ed., *Fault-zone Properties and Earthquake Rupture Dynamics*, Elsevier Academic Press, 2009.

[12] W. H. K Lee, C. M. Valdes, *HYP071PC: A personal computer version of the HYPO71 earthquake location program*, U. S. Geological Survey Open File Report 85–749, 1985.

[13] UNDP/UNESCO, Tables des temps de propagation des ondes séismiques (Hodo-chrones) pour la région des Balkans, Manuel d'utilisation, Strasbourg, 1972.

[14] SORM (Seismological Observatory of the Republic of Macedonia), *Catalogue of earthquakes occurred in 2002 in the Republic of Macedonia and surrounding areas*, Ss. Cyril and Methodius University, Faculty of Natural Sciences and Mathematics, Seismological Observatory, Skopje, 2002.

[15] SORM (Seismological Observatory of the Republic of Macedonia), *Catalogue of earthquakes occurred in 2003 in the Republic of Macedonia and surrounding areas*, Ss. Cyril and Methodius University, Faculty of Natural Sciences and Mathematics, Seismological Observatory, Skopje, 2003.

[16] ISC (International Seismological Centre), *International Seismological Centre Bulletin*, available from <http: //www.isc.ac.uk/>.

[17] R. L. Street, R. B. Herrmann, O. W. Nuttli, Spectral characteristics of the L_g wave generated by Central United States earthquakes, *Geophys. J. Roy. Astron. Soc.*, **41** (1975) 51–63.

[18] R. B. Herrmann, A. Kijko, Modelling some empirical vertical component L_g, *Bull. Seismol. Soc. Am.*, **73** (1983) 157–171.

[19] R. B. Herrmann, An extension of random vibration theory estimates of strong ground motion to large distances, *Bull. Seismol. Soc. Am.*, 75 (1985) 1447–1453.

[20] V. Čejkovska, Empirical relations of seismic moment and earthquake moment magnitude to earthquake local magnitude for the Vardar and West Macedonia seismic zones, *Contributions, Sec. Math. Tech. Sci., MANU*, **XXVII–XXVIII** (2006–2007) 93–115.

[21] L. Pekevski, Q for the territory of Republic of Macedonia, *The Albanian Journal of Natural & Technical Sciences*, **10** (2001) 81–87.

[22] L. B. Kvamme, R. A. Hansen, H. Bungum, Seismic-source and wave-propagation effects of L_g waves in Scandinavia, *Geophys. J. Int.,* **120** (1995) 525–536.

[23] J. Shi, W. Kim, P. G. Richards, The corner frequencies and stress drops of intraplate earthquakes in the northeastern United States, *Bull. Seismol. Soc. Am.*, **88** (1998) 531–542.

[24] J. N. Brune, Tectonic stress and spectra of seismic shear waves from earthquakes, *J. Geophys. Res.*, **75** (1970) 4997–5009.

[25] J. N. Brune, Correction, *J. Geophys. Res.*, **76** (1971) 5002.

[26] J. Havskov, L. Ottemöller, *Seisan: The Earthquake Analysis Software For Windows, Solaris, Linux and Macosx*, *Version 8.2.*, Institute of Solid Earth Physics, University of Bergen, Bergen, 2008.

[27] P. A. Reasenberg, D. Oppenheimer, FPFIT, FPPLOT and FPPAGE: FORTRAN computer programs for calculating and displaying earthquake fault-plane solutions, *U. S. Geological Survey Open File Report*, 85–739, 1985.

Р е з и м е

МЕХАНИЗАМ И ГОЛЕМИНА НА ЖАРИШТЕТО НА ГЊИЛАНСКИОТ (КОСОВСКИОТ) ЗЕМЈОТРЕС ОД 24 АПРИЛ 2002 ГОДИНА СО ЛОКАЛНА МАГНИТУДА $M_L = 5.2$

Гњиланскиот (косовскиот) земјотрес од 24 април 2002 година, со локална магнитуда $M_L = 5.2$, анализиран е најпрво преку инверзија на амплитудниот спектар на поместувањето на брановата група $S_g - L_g$ и одредувањето на *P*-нодалните рамнини. Овде добиените вредности на сеизмичкиот момент, аголната фреквенција на жаришниот амплитуден спектар на поместувањето и Брунова еквивалентна кружна раседна површина за овој земјотрес се, соодветно, $M_0 = 6.48 \cdot 1016$ N·m, $f_0 = 059$ Hz и $\Sigma_{s,eq} = 15.2$ km^2. *P*-нодалните рамнини за четирите најсилни дополнителни земјотреси и распределбата на епицентрите на другите дополнителни земјотреси се исто така одредени, а потоа применети во идентификацијата на вистинскиот жаришен механизам на главниот земјотрес, со една новопредложена метода, која ги вклучува и вертикалните проекции врз Земјината површина на добиената $\Sigma_{s,eq}$ за главниот земјотрес при двете негови *P*-нодални рамнини како можни раседни рамнини. Најдено е дека главниот земјотрес е настанат со нормално десно латерално раседување во рамнина чија трага на Земјината површина има азимут од 238° и која е наклонета под агол

од 22° кон NNW. Се утврди дека ова раседување предизвикало активирања на други раседи и пукнатини како жаришта на значаен број од дополнителните земјотреси. Инаку, ова раседување може да се придружи на тектонски девијаторно напрегнатата раседна структура по должина на реката Биначка Морава, чија долина започнала да тоне изразито кон крајот на горниот плиоцен односно на почетокот на квартерот.

Клучни зборови: сеизмички циклус, ломење, механизам на земјотресното жариште, раседување, сеизмички момент, големина на раседната површина, аголна фреквенција.

Adress:

Vera Čejkovska
Ss. Cyril and Methodius University in Skopje
Faculty of Natural Sciences and Mathematics
Seismological Observatory
Mariovska 3,,
PO Box 422, MK–1001 Skopje
Republic of Macedonia
v.cejka@gmail.com

Lazo Pekevski
Ss. Cyril and Methodius University in Skopje
Faculty of Natural Sciences and Mathematics
Seismological Observatory
Mariovska 3,
PO Box 422, MK–1001 Skopje
Republic of Macedonia
lazopekevski@yahoo.com

Dragana Černih
Ss. Cyril and Methodius University in Skopje
Faculty of Natural Sciences and Mathematics
Seismological Observatory
Mariovska 3,
PO Box 422, MK–1001 Skopje
Republic of Macedonia
dcernih@yahoo.com

APPENDIX

Locations and local magnitudes (M_L) obtained at the Seismological Observatory in Skopje (SKO, 41.97°N, 21.44°E) for the events of the 24 April 2002 M_L 5.2 Gnjilane earthquake sequence in the period 24 May 2002 – 22 June 2003. H and h – hypocentral time and depth, φ and λ – epicentral latitude and longitude

No.	Date D M Y	*H* (GMT) h : min : s	φ °N	λ °E	*h* km	M_L
1.	24.04.2002	10:51:51.11	42.42	21.52	15.0	5.2
2.	24.04.2002	11:06:07.48	42.42	21.53	17.5	3.5
3.	24.04.2002	11:08:01.96	42.41	21.58	20.1	3.4
4.	24.04.2002	11:08:02.17	42.42	21.53	16.0	0.9
5.	24.04.2002	11:10:55.79	42.42	21.52	17.0	2.4
6.	24.04.2002	11:17:46.47	42.43	21.53	20.4	3.7
7.	24.04.2002	11:24:22.20	42.43	21.51	18.0	4.1
8.	24.04.2002	11:33:14.88	42.44	21.50	16.3	3.9
9.	24.04.2002	12:47:13.27	42.39	21.66	12.2	1.7
10.	24.04.2002	14:18:58.96	42.42	21.53	13.3	1.9
11.	24.04.2002	14:28:05.25	42.28	21.63	20.0	2.2
12.	24.04.2002	14:45:37.98	42.44	21.53	13.5	2.0
13.	24.04.2002	16:04:29.36	42.45	21.53	16.7	3.9
14.	24.04.2002	16:33:23.22	42.43	21.53	16.4	2.2
15.	24.04.2002	17:09:05.03	42.44	21.56	17.7	2.4
16.	24.04.2002	23:37:57.46	42.44	21.54	20.0	4.1
17.	24.04.2002	23:59:16.93	42.44	21.51	16.8	2.4
18.	25.04.2002	00:28:02.91	42.43	21.50	24.0	2.1
19.	25.04.2002	00:47:53.37	42.29	21.52	21.1	2.0
20.	25.04.2002	02:04:08.60	42.34	21.57	18.8	2.1
21.	25.04.2002	02:04:55.05	42.32	21.53	21.7	2.1
22.	25.04.2002	03:43:34.81	42.45	21.51	18.2	4.1
23.	25.04.2002	03:48:37.90	42.44	21.57	17.3	2.6

No.	Date D M Y	H (GMT) h : min : s	φ °N	λ °E	h km	M_L
24.	25.04.2002	11:56:48.48	42.44	21.54	16.0	2.6
25.	25.04.2002	13:35:01.62	42.33	21.65	15.3	1.7
26.	26.04.2002	00:21:31.70	42.42	21.47	12.0	4.1
27.	26.04.2002	00:27:05.13	42.31	21.60	19.3	2.1
28.	26.04.2002	03:13:58.27	42.38	21.59	12.2	1.4
29.	26.04.2002	05:57:14.24	42.39	21.54	11.9	3.0
30.	26.04.2002	06:13:48.06	42.41	21.53	18.3	3.0
31.	26.04.2002	06:16:18.95	42.44	21.54	16.0	3.0
32.	26.04.2002	06:31:03.60	42.44	21.52	18.1	3.7
33.	26.04.2002	07:00:40.31	42.43	21.52	11.2	3.3
34.	26.04.2002	10:10:58.11	42.44	21.55	13.9	0.9
35.	26.04.2002	12:42:04.11	42.44	21.55	18.0	3.5
36.	26.04.2002	13:06:08.49	42.33	21.63	18.0	2.3
37.	26.04.2002	14:14:03.33	42.44	21.54	17.8	3.6
38.	26.04.2002	18:55:02.93	42.36	21.62	15.5	2.0
39.	27.04.2002	04:09:21.55	42.45	21.53	11.2	2.0
40.	27.04.2002	10:16:13.45	42.43	21.55	16.0	2.7
41.	27.04.2002	14:55:39.14	42.42	21.56	16.0	2.4
42.	27.04.2002	22:23:44.69	42.44	21.56	14.4	2.4
43.	28.04.2002	02:30:36.82	42.42	21.63	16.0	3.6
44.	28.04.2002	12:09:26.53	42.45	21.54	16.6	2.8
45.	29.04.2002	02:12:12.07	42.31	21.65	15.7	2.3
46.	29.04.2002	04:39:47.66	42.45	21.47	15.5	3.5
47.	29.04.2002	05:08:06.40	42.34	21.56	16.0	2.0
48.	29.04.2002	06:21:05.05	42.32	21.64	17.2	2.1
49.	29.04.2002	10:10:52.28	42.44	21.55	19.8	4.0
50.	29.04.2002	13:58:41.68	42.45	21.54	16.0	2.6
51.	29.04.2002	15:53:21.17	42.35	21.59	19.0	2.6
52.	29.04.2002	16:16:13.15	42.34	21.60	25.8	1.9

No.	Date D M Y	H (GMT) h : min : s	φ °N	λ °E	h km	M_L
53.	01.05.2002	06:03:02.09	42.42	21.50	17.2	2.5
54.	01.05.2002	23:46:50.66	42.43	21.53	11.6	2.4
55.	02.05.2002	03:31:30.53	42.42	21.53	16.0	4.0
56.	02.05.2002	07:31:59.61	42.46	21.48	16.0	3.3
57.	02.05.2002	20:13:37.97	42.38	21.53	18.7	3.2
58.	04.05.2002	21:56:32.85	42.43	21.52	15.4	2.1
59.	05.05.2002	15:02:07.25	42.39	21.53	14.4	2.0
60.	05.05.2002	16:06:40.22	42.39	21.51	17.9	3.4
61.	06.05.2002	13:29:12.50	42.39	21.51	16.7	3.6
62.	08.05.2002	03:45:14.94	42.39	21.53	16.6	3.5
63.	08.05.2002	13:58:01.15	42.44	21.55	17.9	2.2
64.	17.05.2002	02:45:34.28	42.42	21.49	16.0	2.3
65.	20.05.2002	18:09:43.95	42.45	21.54	14.8	2.4
66.	13.06.2002	08:27:17.45	42.44	21.53	17.5	3.4
67.	13.06.2002	08:41:57.43	42.45	21.54	17.0	3.3
68.	14.06.2002	03:05:59.56	42.44	21.52	17.5	3.3
69.	14.06.2002	23:04:14.66	42.44	21.53	16.9	3.1
70.	16.06.2002	22:09:40.71	42.39	21.53	18.0	3.2
71.	03.07.2002	22:48:14.41	42.48	21.51	5.9	2.3
72.	22.07.2002	13:25:51.04	42.40	21.47	10.0	2.0
73.	29.11.2002	05:25:41.20	42.26	21.33	10.0	2.0
74.	25.03.2003	19:02:00.08	42.43	21.52	12.1	2.8
75.	27.03.2003	05:04:35.38	42.41	21.47	10.0	2.3
76.	27.03.2003	05:07:10.70	42.42	21.52	17.0	2.6
77.	28.03.2003	06:30:24.50	42.43	21.53	16.6	2.7
78.	31.05.2003	05:38:22.88	42.27	21.38	17.3	2.0
79.	20.06.2003	23:39:08.68	42.23	21.28	19.6	2.3
80.	22.06.2003	05:39:42.00	42.45	21.39	15.0	2.3